

1

The ERL Project

1-1 Introduction

The energy recovery linac (ERL) being developed at KEK can help usher in a new era in materials science. Illumination of a specimen with a short, coherent, nanometer-wide X-ray beam will enable scientists to perform nondestructive measurements on rapidly evolving dynamic materials and microorganisms with a nanometer-scale spatial resolution. This would benefit research for a host of applications in materials, life, chemical, and environmental sciences. Some interesting examples of these applications include the development of next-generation high-speed communication devices and catalysts that enable the generation of clean hydrogen energy, as well as other applications for drug-discovery research, sub-cellular imaging, and efficient light energy utilization.

Because a GeV-class ERL machine has not been constructed anywhere in the world, it is necessary to first construct a compact ERL (cERL) with an energy of 35–200 MeV that can be used for the development of several critical accelerator components such as a high-brilliance DC photocathode electron gun and superconducting cavities for the injector and main accelerator.

On April 22, 2010, we establish a review committee on the cERL to examine the feasibility of constructing a cERL from the view points of technologies, budget, and manpower (Fig. 1). The committee members were K. Oide (KEK) (Chair), N. Kumagai (RIKEN), S. Yamaguchi (KEK), M. Kato (UVSOR), A. Enomoto (KEK), H. Hanaki (JASRI), K. Akai (KEK), and H. Kobayashi (KEK). The discussions at the meeting were summarized as follows: “It is a reasonable target to construct a cERL of 35 MeV, 10 mA, and an emittance of 1 mm-mrad in the first stage. There are no significant problems associ-



Figure 1
Photograph of the review committee of cERL, established on April 22, 2010.

ated with the budget profile, manpower, and technical developments to achieve the above target by the end of the fiscal year 2012.” The report of the review committee can be referred to on the Web site http://pfwww.kek.jp/ERLoffice/erl_hyouka/index.html (in Japanese). Then, we focused our attention on constructing a cERL during 2010. Details on the construction of the cERL are described in the next section.

Furthermore, it is important to examine the possibility of achieving cooperation between the ERL project office and the LC project office for arriving at the same targets of development of the accelerator. It is clear that both the offices promote the development of future accelerators based on the super-conducting RF cavities. Even though each project requires a different mode of operation (CW and pulse mode of operation) of the accelerator, we have tried to find common ground for both projects. On December 24, 2010, we established a committee under the leadership of Dr. S. Yamaguchi (project leader of the LC project office) to discuss the items. Its findings will be published in the next Annual Report.

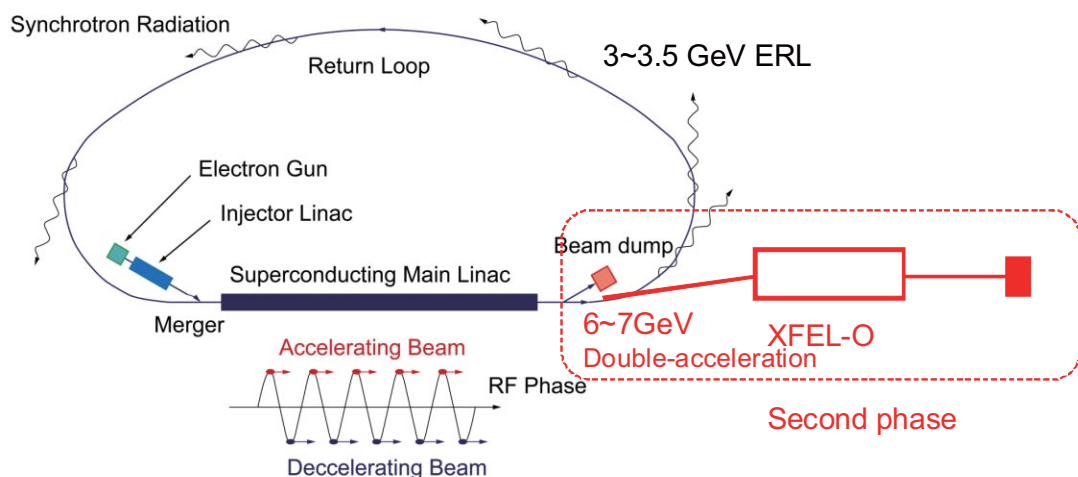


Figure 2
Schematic view of the steps involved in the development of the 3-GeV-class ERL. The fabrication of the 3-GeV-class ERL will be completed in the first phase, and the XFEL-O will be constructed in the second phase.



Figure 3
Photograph of Dr. Yuri Shvyd'ko (APS) at the IMSS symposium.



Figure 4
Photograph of Dr. G. Lawrence Carr (BNL) at the JSSRR conference.

On February 23, 2011, we established a steering committee for the ERL project office and received a very important directive: “you should take into accounts the future development of the insertion device technologies.” This comment means that the possibilities to realize much shorter period of the undulator gives us the reconsideration about the beam energy to minimize the construction budget for future light source. On the basis of this directive, we have modified the specifications of the ERL to be constructed in the first phase (as shown in Fig. 2) from a 5-GeV-class ERL to a 3-GeV-class ERL. The details of this modification will be conveyed to all synchrotron radiation users at the ERL science workshop II, which is scheduled in the end of April 2011.

We invited Dr. Yuri Shvyd'ko (APS) and Dr. Alfred Baron (RIKEN) for the IMSS symposium in December 2010 to provide scientific updates. Dr. Yuri Shvyd'ko (Fig. 3) explained the development of the diamond crystal X-ray optics for an X-ray free electron laser oscillator (XFEL-O). He concluded that while there are several challenges to be met, there are no critical problems associated with the fabrication of XFEL-O, provided the beam can be prepared as per specifications. Dr. Alfred Baron presented a vision for the future applications, which will be realized by XFEL-O based on flux-oriented high-resolution X-ray inelastic scattering. Furthermore, at the Japanese Society for Synchrotron Radiation Research (JSSRR) conference in January 2011, Dr. G. Lawrence Carr (BNL) (Fig. 4) explained the application

of coherent terahertz radiation based on the accelerator and the cERL.

On March 11, 2011, a major earthquake hit east Japan. Although several accelerator components and experimental apparatuses in KEK were damaged, there were no serious damages for the ERL accelerator development. Therefore, we can retain the end of FY2012 as the target date for the successful operation of the cERL.

1-2 Progress Achieved in 2010

ERL project to develop 3-GeV class ERL

As previously mentioned, we decided to change the operational energy of the ERL from 5 GeV to 3 GeV. Figure 2 shows the schematic of the device as planned. As the first stage, 3-GeV-class ERL will be constructed for the experiments by means of high brilliant soft X-ray and hard X-ray with sub-pico second pulsed synchrotron radiation. The advantages of changing the operational energy are as follows. The first advantage is that a wide variety of user demands can be accommodated, such as the need to use soft X-ray for spectroscopy measurements for investigating the electron states in materials and the need to use coherent hard X-ray imaging for investigating the electron structure in materials. Because the ERL project will be an alternative facility to the 2.5-GeV PF ring and given the fact that there are no 3-GeV-class high-brilliance synchrotron radiation facilities in Japan, This advantage is important for KEK. The second advantage is that the construction and running cost are reduced. The third advantage is that an accelerator with a single loop and not a double loop can be designed; this design is simpler than that of the previous 5-GeV accelerator. The disadvantages are (1) the emittance value is slightly higher (15–17 pm-rad) than that expected from the 5-GeV-class ERL (10 pm-rad) and (2) it is difficult to achieve the X-ray undulator light at the first harmonics. However, both these disadvantages are not serious for the project, especially since the latter will be negated by advancement of the undulator technology that will enable the realization of a much shorter period undulator.

As shown in Fig. 2, the 6–7-GeV XFEL-O will be constructed in the second phase. The 3-GeV-class ERL can automatically produce sufficiently high quality electron beams to enable the operation of the XFEL-O with double acceleration by using the former constructed ERL accelerator. Thus, the second phase of construction can be completed with the construction of a 50–60-m undulator and an X-ray resonator using diamond crystal optics.

Renovation and clean-up of the ERL Test Facility for the construction of the cERL

As mentioned previously, we are constructing the cERL in the ERL Test Facility (previously known as the



Figure 5
Schematic of the cERL as expected at the end of FY 2012.



Figure 6
View of the ERL Test Facility after renovation.

East Counter Hall) at KEK. The first objective of the cERL is to demonstrate the ERL operation of generating low-emittance (normalized emittance: $1 \text{ mm} \cdot \text{mrad}$) beams of 10 mA (CW) at a beam energy of 35 MeV. For this purpose, we will construct a 5-MeV injector linac, a main linac having two 9-cell cavities in a single cryostat, and a single return loop, as shown in Fig. 5, by the end of FY2012. Once the first objective is achieved, we intend to upgrade the cERL in a step-by-step manner. In future, we intend to increase the beam current up to 100 mA and install additional cavities in the main linac.

The ERL Test Facility (ETF) was used for high-energy experiments and nuclear physics experiments using proton beams from a 12-GeV proton synchrotron. Because these facilities are being shifted to the J-PARC site, the hall housing them is being used for constructing a cERL. In 2009, approximately 10,000 tons of concrete shielding as well as old proton beam lines with activated components were removed from the EDB (Fig. 6). Additionally, a cooling water plant and an electrical substation were also renovated for incorporation as infrastructure for the cERL.

In 2010, after clearing the old proton beam lines, we discovered large iron plates that were attached to the floor and were slightly activated. Moreover, two cable pits filled with many cables, iron pipes, and polyethylene beads for neutron shielding were also discovered. This



Figure 7
Photograph showing the activated materials to be collected from the pits.

radioactive matter weighs approximately 30 tons. In order to construct the radiation shielding for the cERL, we decided to take away these activated fillings safely (Fig 7). Iron plates with a thickness of 9 mm and an area of 150 m^2 were cut into small pieces with an area of 1 m^2 , and each piece was checked whether it was activated or not. The materials in the two pits were handled and checked similarly. The designing of the concrete shielding for the cERL and the cleaning of the hall started simultaneously. Renovation of the ETF was completed, and the radiation shielding will be constructed in 2011.

R&D efforts for the ERL project

High-brightness DC photocathode gun and gun test beamline

Two high-brightness DC photocathode gun systems at JAEA and KEK are being developed jointly by JAEA, KEK, Hiroshima University, Nagoya University, and Yamaguchi University.

In 2009, the first gun at JAEA could be successfully operated at a voltage of 500 kV with a cathode support. Currently, the gun is operated at a cathode electrode voltage of up to 380 kV and can extract a test beam current of $5.7 \mu\text{A}$ at a gun voltage of 300 kV. The base pressure of the gun was lowered to $1 \times 10^{-9} \text{ Pa}$ using an 18,000 L/s non-evaporable getter pump. A preparation to extract a high average current beam at a gun voltage of 500 kV is in progress.

The main titanium chamber and a pair of segmented insulators for the second gun at KEK were fabricated in 2009. These vacuum parts were baked, and a total outgassing of $4.6 \times 10^{-11} \text{ Pa} \cdot \text{m}^3/\text{s}$ and $4.0 \times 10^{-10} \text{ Pa} \cdot \text{m}^3/\text{s}$ from these parts was measured. The second gun is under construction, after which it will be prepared to apply high voltage.

A beam diagnosis system using a 200-kV DC gun was constructed at KEK to evaluate the intrinsic thermal emittance and the temporal response of a semiconductor cathode. At present, a cathode for the ERL is under development with the combined effort from Nagoya University. An original NPES3 beamline consisting of sole-

noid magnets, profile monitors, and a beam dump was used in the first operation to test the NPES3 200-kV DC gun system. Since September 2010, we have changed the beamline from the original NPES3 to a new gun test beamline, which consists of solenoid magnets, profile monitors, a double slit system to measure emittance, a deflecting cavity system to measure the time response of the cathode, and a beam dump. Figures 8 and 9 show the photograph of the new beam line and the layout, respectively. After tuning the solenoid magnets and the corrector magnets, we transferred more than 95% of

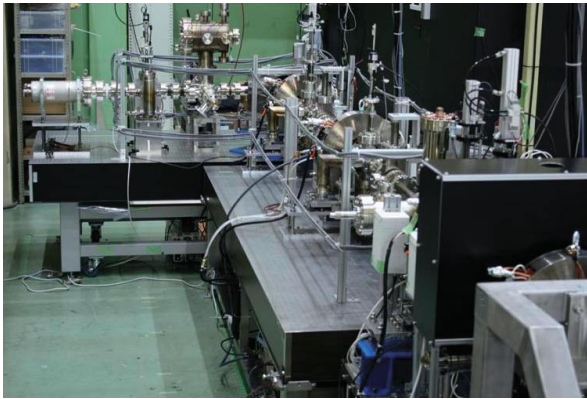


Figure 8
Photograph of the gun test beamline in the AR south experimental hall.

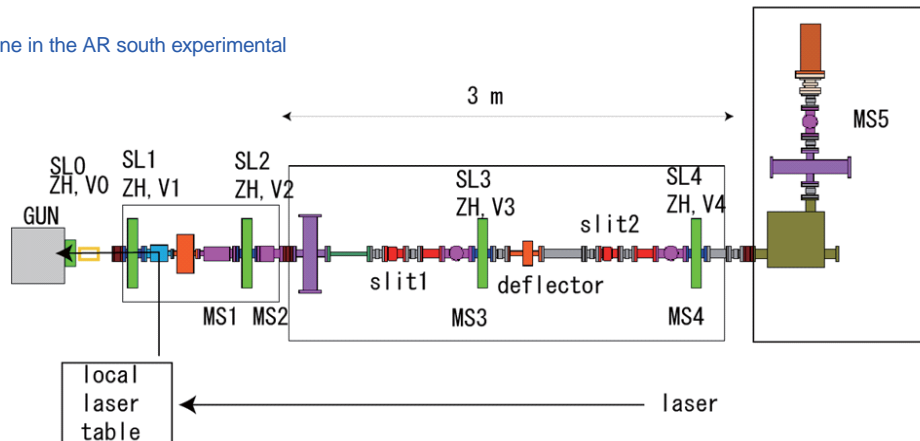


Figure 9
Layout of the gun test beamline.

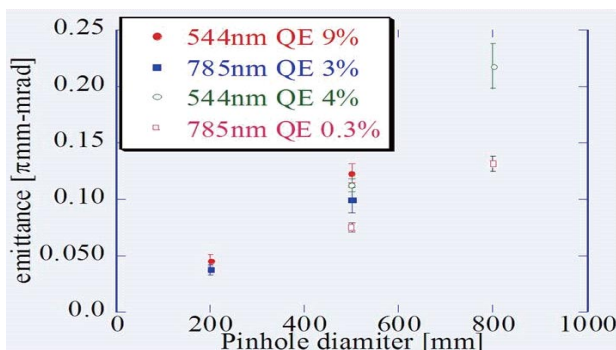


Figure 10
Preliminary results of the transverse emittance generated by the bulk GaAs cathode with drive laser wavelengths of 544 nm and 785 nm. The horizontal axis denotes the pinhole diameter, which corresponds to the radius of the laser on the cathode surface, and the vertical axis denotes the measured transverse emittance. The quantum efficiency was varied in the measurements.

the beam from the gun to the beam dump with a 100-kV gun voltage and a 10-nA beam current. To investigate the properties of the cathode materials, transverse emittance and time response have been measured using the new beamline. Figure 10 shows the preliminary result of the transverse emittance of the electron beam, which is generated by a bulk GaAs cathode. In addition, we measure the properties of superlattice cathodes.

Drive lasers

The drive laser system has to provide a continuous pulse train at a 1.3-GHz beam repetition rate with enough average power at the matched wavelength of the photocathode. In order to achieve the first milestone of realizing a 10-mA beam operation, it should be noted that the drive laser system is required to have an average power of 1.5 W at a wavelength of 530 nm when the quantum efficiency is assumed to be 1.5% (in future, in order to realize a 100-mA beam operation, power with a higher order of magnitude will be required.). The strategy of development is shown in Fig. 11(a).

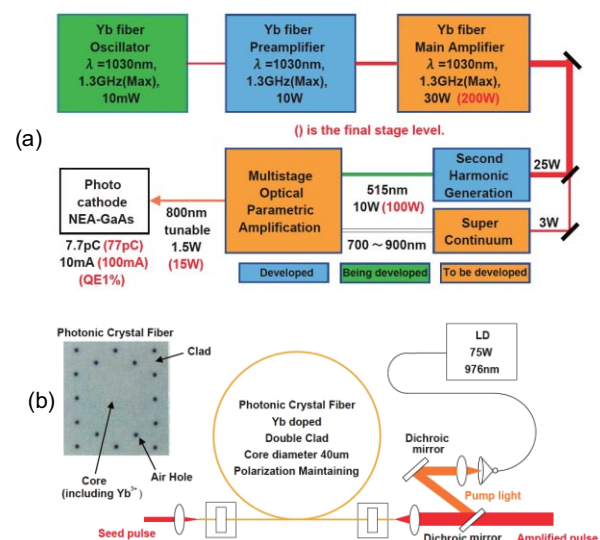


Figure 11
(a) Strategy for the development of the drive laser system, (b) system of the high-power amplifier utilizing an Yb-doped photonic crystal technique for producing an average power of 30 W at the fundamental wavelength.

Development work has been carried out in collaboration with AIST and ISSP [1]. It should be noted that strategies to develop a fiber oscillator, to generate second harmonics, to develop a high-power amplifier, and to convert the wavelength via super-continuum generation have been studied separately. There have been improvements in the strategies used to develop the oscillator to enable higher repetition and noise reduction, and a 421-MHz oscillator that suppresses a super-mode noise to lower than -30 dB has been realized. Second harmonic generation with a conversion efficiency of 49% has been confirmed with a fundamental power of 10 W at a repetition rate of 85 MHz and a pulse duration of 1 ps. The high-power amplifier utilizing a Yb-doped photonic crystal technique has succeeded in producing an average power of 30 W at the fundamental wavelength, as shown in Fig. 11(b). Production of light with a wavelength of 800 nm has been demonstrated with a high non-linear photonic crystal via super-continuum generation.

SC Cavities for the Injector

An injector cryomodule, which includes three 2-cell SC cavities, is required to accelerate CW electron beams of 100 mA from 0.5 MeV to 10 MeV. The targeted accelerating gradient and the transmission power



Figure 12
One of three 2-cell SC cavities for an injector cryomodule.

through each input coupler are 14.5 MV/m and 170 kW, respectively. A completed 2-cell SC cavity for the injector cryomodule is shown in Fig. 12. The 2-cell cavity has two input-coupler ports and five loop-type HOM couplers. A slide-jack tuner with a pair of piezo elements is attached at the thick titanium base-plates for a frequency tuning system. Vertical testing of three cavities is scheduled to qualify their cavity performance before assembly of the cryomodule. Conditioning of two prototype input couplers was carried out in a high power test stand with a CW 300 kW klystron at ETF, as shown in Fig. 13. These couplers were successfully conditioned with a peak RF power of 180 kW in a pulsed operation (0.2 s and 0.5 Hz) and a CW RF power of 50 kW. Six input couplers for the injector cryomodule are under fabrication.

SC cavities for main linac

The second 9-cell cavity of the ERL model-2 shape was fabricated and measured to establish the fabri-

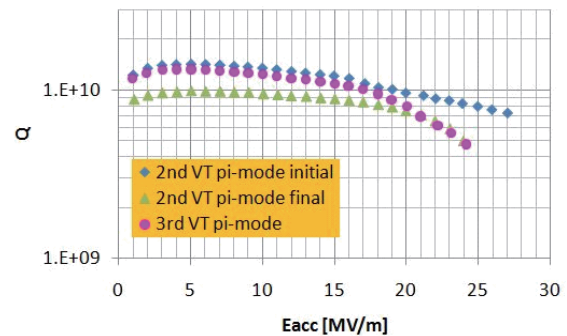
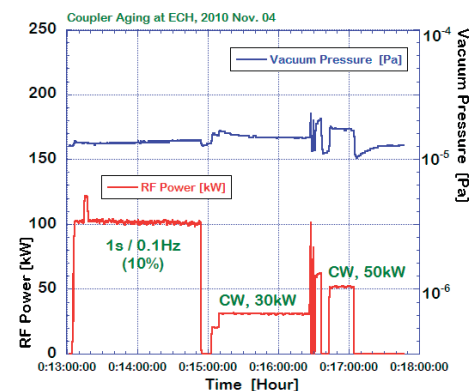


Figure 14
Performance of the test cavity. Initial performance was degraded by RF conditioning (2nd-final); however, it was recovered by heating the test cavity to room temperature. Strong electron emission caused by the conditioning could not be eliminated by the heating (3rd).



Figure 13
A high-power test stand for input couplers at the ECH (left) and the data logged for RF power and vacuum pressure during RF conditioning (right).



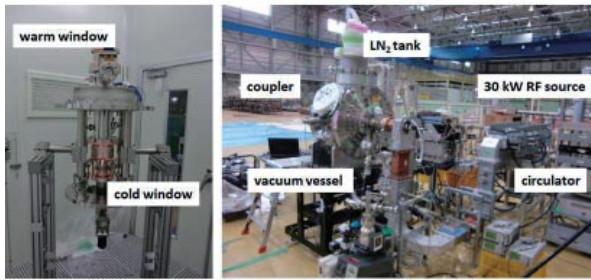


Figure 15
Coupler and cold test assembly. The test coupler was cooled with Liquid N₂ in the vacuum vessel and powered to 25 kW while monitoring the increase in temperature of the bellows in the inner and outer conductors.

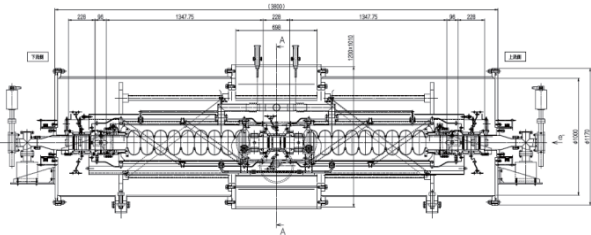


Figure 16
A schematic of a prototype cryomodule. Two 9-cell cavities inserted in 2-K He jackets are connected together with the HOM dampers, which are cooled by Liquid N₂. The total heat load including an RF dynamic loss is estimated as 100 W at 2 K.

cation process and its parameters. The accelerating gradient reached 23 MV/m at the first cold test, which was greater than the desired gradient of 20 MV/m. However, RF processing at a higher gradient of 28 MV/m produced strong electron emission in the cavity and degraded both Q and the maximum gradient, as shown in Fig. 14.

A prototype input coupler was powered to 25 kW under full reflection monitoring of the temperature of the bellows parts of the inner and outer conductors (Fig. 15). The inner and outer conductors were cooled by gas N₂ and liquid N₂, respectively, so as to simulate the conditions in the cryomodule. The increase in temperature of these bellows was within acceptable limits when power was maintained at 20 kW for 16 h.

Heat conduction measurement of a higher order mode (HOM) damper and the mechanical performance test of a prototype frequency tuner are in progress. The design of a cryomodule including two 9-cell cavities and the above-mentioned components is underway (Fig. 16).

RF sources (HLRF)

The prototype input couplers for the injector were successfully tested at a high power of 150 kW CW using a 300-kW CW klystron and a 150-kW circulator at the PF Power Supply Building. Then, the RF system for the injector was moved to the ETF and installed there where amenities such as electricity and a water cooling system were provided. High-power tests up to 280 kW were performed using the power supply unit, which was



Figure 17
300-kW klystron system installed in the ERL Test Facility.

manufactured in FY2009.

We have prepared two RF sources for the main linac of the cERL, namely, a 30-kW induction output tube (IOT), i.e., VKL-9130 from CPI, and a 35-kW klystron, i.e., E3750 from Toshiba. Two old power supply units for these sources were transferred from JAEA, and a new power supply that was manufactured in FY 2009 was installed in the ETF. The IOT high-power test was performed up to 30 kW using one of the transferred power supply units. A high-power test of the power supply unit manufactured in FY2009 was performed using a resistive load; the result of this test confirmed that the power supply unit met the required specification. The design of the layout of the RF source of the cERL was completed. The 300-kW klystron system installed in the ETF is shown in Fig. 17.

RF sources (LLRF)

cERL operations require RF stabilities of 0.1% in amplitude and 0.1° in phase. In order to satisfy these requirements, a digital low-level RF (LLRF) system has been developed on the basis of the previous experience at STF in KEK [2].

A micro-TCA system, which is widely used in the telecommunication industry and has high availability, is adopted for digital control. The micro-TCA board consists of a base card having one field-programmable gate array (FPGA) and daughter cards with analog to digital converters (ADCs) and digital to analog converters (DACs), as shown in Fig. 18. Parameter setting or

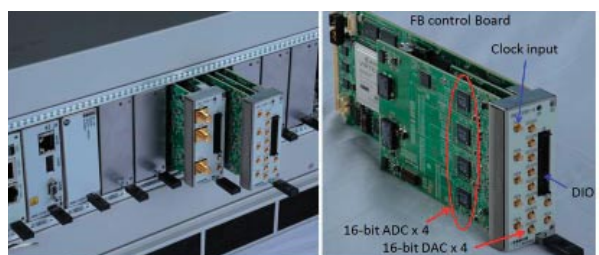


Figure 18
Micro-TCA chassis (left) and micro-TCA board (right) for the digital feedback system.

data acquisition is carried out through the giga-bit ethernet bus at the backplane. An experimental physics and industrial control system (EPICS) is selected as the communication protocol. A special FPGA (Virtex-5 FXT by Xilinx) having a hardcore CPU (power PC) is selected in order to install EPICS on the board. Thus, each board becomes an EPICS-IOC [3]. An ADC card and a DAC card used as the daughter cards are attached to the base card. The ADC card is equipped with four 16-bit ADCs and the clock input. Similarly, the DAC card is equipped with four 16-bit DACs [4]. Evaluation of the entire digital system is scheduled in 2011.

Cryogenic systems

According to the High Pressure Gas Safety Act of Japan, the helium cryogenic system of the cERL should pass the completion inspection by Ibaraki prefecture before the commencement of the regular operation of the system. The system passed the completion inspection in August 2010, without any problem, and regular operation of the cryogenic system has been authorized by the prefecture.

Because the helium liquefier/refrigerator (the blue machine shown in the center of Fig. 19) was moved from another institute after a long-term operation, it was highly possible that the helium lines in the refrigerator might be contaminated with oil from helium circulation compressors. Such contamination can choke the flow of helium in them when the oil freezes. Additionally, the contamination of helium lines with the oil may decrease the heat exchange rate in heat exchangers. Therefore, to ensure the performance of the helium refrigerator, we attempted to remove as much oil as possible from the helium lines. After the completion of inspection, we commissioned the refrigerator and successfully produced liquid helium in January 2011. The production rate of liquid helium was found to be approximately 250 L/h of the specification value. The produced liquid helium is stored in a 3000-L Dewar (a white storage vessel seen on the left end of the photograph).



Figure 19
Helium liquefier/refrigerator that is installed in ERL Test Facility.

cERL magnet systems

A sector-type bending magnet for the recirculation path of the cERL was designed and manufactured. The main parameters of this magnet are listed in Table 1 and its photograph is shown in Fig. 20. The magnet is fabricated by lamination of adhesive silicon steel sheets with a thickness of 0.5 mm. The rectangular magnetic core was cut to exhibit a trapezium shape after the laminated steel sheets were baked for thermocompression bonding. The beam energy will be increased from 35 MeV to 245 MeV in a step-by-step manner at each construction phase. The good field region of the bending magnet should be horizontally wide owing to the large bending angle of the wide beam energy range. Therefore, silicon steel having high permeability in a small magnetic field was adopted; $\mu_s > 5000$ at $B \sim 0.1$ T.

Table 1 Principal parameters of the magnet.

Magnet core shape	Sector (trapezium)	
Core cross section shape		C
Minimum vertical pole gap	mm	58
Horizontal pole width	mm	230
Turn number of the coil	tums	56
Silicon steel thickness	mm	0.5
Silicon steel material	50H250 (NIPPON STEEL CO.)	
Design current	A	752
Design voltage	V	20
Maximum beam energy	MeV	245



Figure 20
Photograph of the magnet for the cERL.

Schedule

The schedule for constructing the cERL and the 3-GeV-class ERL is shown in Fig. 21. Fabrication of the accelerator components will be carried out from 2010 to the middle of 2012. We will start the testing of the components of each accelerator soon after their installation, and subsequently, we will start the beam operations at

the end of FY2012 at an accelerated energy of 35 MeV. The beam test will provide important information on whether further improvement in the components is necessary, as well as information on the drawbacks of the design of the 3-GeV-class ERL. The construction of the 3-GeV-class ERL will start in 2015, and the user operation will start from 2020.

REFERENCES

[1] I. Ito, N. Nakamura, Y. Honda, Y. Kobayashi, K. Torizuka and D. Yoshitomi, *Proc. IPAC (2010)* TUPD104.
 [2] S. Michizono, S. Fukuda, H. Katagiri, T. Matsumoto, T. Miura, Y. Yano and Y. Okada, *Proc. PAC (2009)*, WE5PFP083.
 [3] J.-I. Odagiri, K. Akai, K. Furukawa, S. Michizono, T. Miura, T.T. Nakamura, H. Degushi, K. Hayashi, J. Mizuno and M. Ryoshi, *Proc. IPAC (2010)* WEPEB003.
 [4] T. Miura, A. Akiyama, D.A. Arakawa, S. Fukuda, H. Katagiri, T. Matsumoto, S. Michizono, J.-I. Odagiri and Y. Yano, *Proc. IPAC (2010)* TUPEA048.

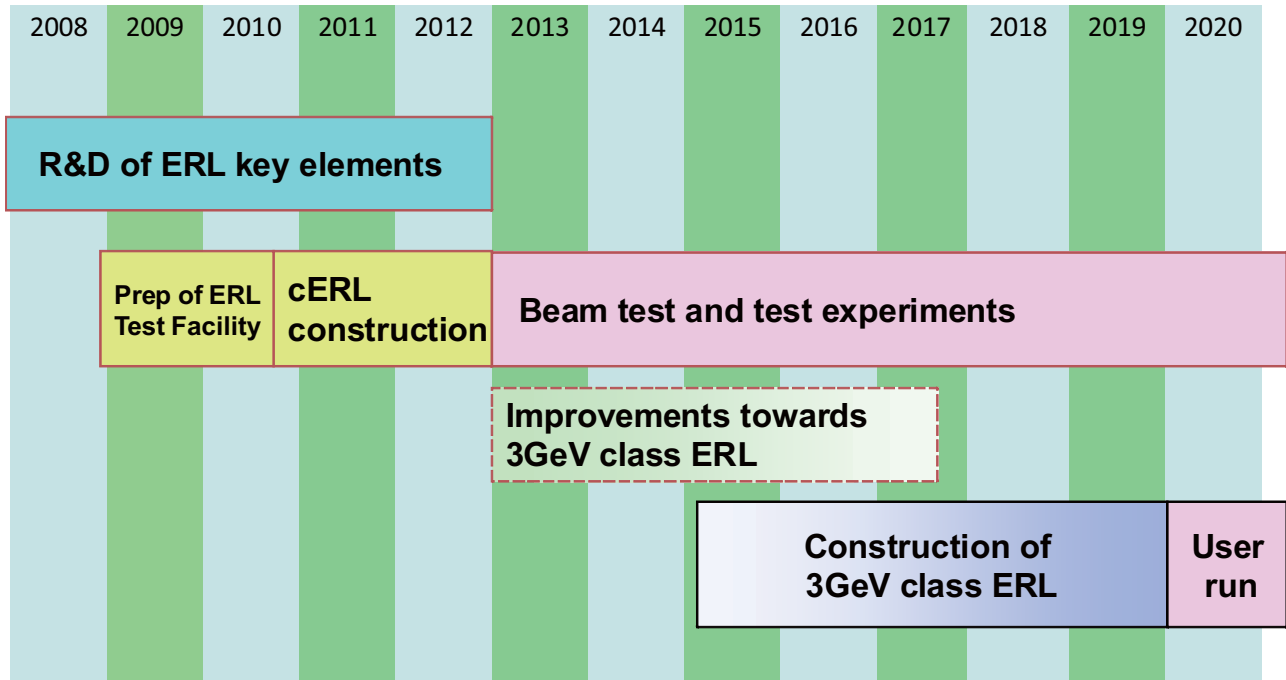


Figure 21
Time schedule of the ERL project.